Child Occupant Protection in ISOFIX CRS

Jia Hu[1,2], Koji Mizuno[2]

(1.College of Mechanical and Automotive Engineering, Hunan University, Changsha, Hunan 410082, China; 2.School of Engineering, Nagoya University, Furo-cho, Chikusa-ku, Nagoya 4648603, Japan)

Abstract: ISOFIX child restraint system (CRS) implements a simple, rigid and standardized attachment to vehicle seat as compared to the conventional type CRS installed by vehicle seat belt. However, it was found that except head excursion other injury criteria for a child seated in an ISOFIX CRS were comparable to those in the conventional type of 5-point harness CRS. In this research, an FE model of a Hybrid III 3YO dummy and a 3-year-old child human model positioned in the conventional type 5-point harness CRS (using vehicle seat belt for installation) and ISOFIX CRS were developed and validated using frontal sled tests. The behavior and biomechanical responses of the Hybrid III dummy model and the child human FE model were compared and analyzed. A top-tether force limiter was proposed to reduce the loadings to the head, neck and chest of a child positioned in the ISOFIX CRS. For evaluating the effectiveness of the top-tether force limiter, FE simulations for two conditions, CRS in proper use and CRS harness having slack, were performed. Ridedown and restraint energy and the restraint energy related with the CRS harness and the CRS installation systems for the chest of the Hybrid III dummy and child human FE model were analyzed and compared between the conventional type of 5-point harness CRS and the ISOFIX CRS in different using conditions. The results show that the energy absorbed by the CRS harness is comparable between the conventional type of 5-point harness CRS and the ISOFIX CRS, and consequently the chest acceleration levels are comparable between the two types of CRSs. The top-tether force limiter is shown to be effective on reducing head and chest accelerations and upper neck force and moment.

Key words: ISOFIX CRS, child human FE model, Hybrid III 3YO dummy, upper neck, chin-chest contact, energy efficiency.

1 INTRODUCTION

Traffic accidents are one of the significant factors causing children fatalities. Research on the effectiveness of child restraint systems (CRSs) has found them to reduce the risk of fatal injury by 71 percent for infants (less than 1 year old) and by 54 percent for toddlers (1-4 years old) in passenger cars [1]. However, surveys on CRSs using condition reveal that CRSs are frequently misused [2, 3, 4]. ISO (International Organization for Standardization) started a project of CRS anchorage system in 1990 with misuse reduction as the major target, which was called ISOFIX system [5]. As the CRS is anchored in the vehicle seat by two rigid anchorages (2-point rigid ISOFIX-system), the ISOFIX CRS can be attached to the vehicle seat rigidly. To limit the pitch motion of the ISOFIX CRS, some anti-rotational devices are required. For a forward-facing ISOFIX CRS, a top tether anchoring in the head region of the backrest of the CRS is used as an additional installation measure [5, 6]. Besides the CRS installation problems, whether a child is secured in the CRS seat fitly or tightly enough is also an important factor which will influence the complete potential offered by the ISOFIX CRS being exhausted fully in a crash [6].

Statistical data of motor vehicle related accidents showed that the most frequent injured body region for children is the head in frontal or side crashes [7]. However, as a small child has a large head mass and a fragile neck structure [8], the loading to the neck will probably cause a severe or fatal injury, which had been revealed in real-world accidents [8, 9]. De Jager et al. [10] have also indicated that the neck is an important area to protect for children (younger than 4 years of age) in forward facing CRS, even if these injuries are not very frequent.

Keller and Mosdal [11] had elucidated that better restraint of the torso would be expected to result in the deceleration forces being transferred to the unrestrained cervical spine and head. A force-limiting device is originally designed for a three-point belt system to reduce the shoulder belt load applied to an adult at the expense of allowing additional excursions of the head and thorax in real-world crashes [12, 13]. Van Rooij et al [12] had applied a force-limiting device to the vehicle seat belt which was used to secure a Hybrid III 6YO dummy to a booster seat, and the results showed that the force-limiting device was effective on reducing injury peak values but a high injury peak duration.

ISOFIX system is a rigid anchorage system, which can limit the CRS forward movement in a frontal crash, and consequently child head forward excursion can be reduced compared with the conventional type CRS installed by vehicle seat belt. However, it was found that except head excursion other injury criteria for a child seated in a 5-point harness ISOFIX CRS were comparable to those in the 5-point harness conventional type CRS [14]. In the present research, an FE model of a Hybrid III 3YO dummy and a 3-year-old child human model positioned in the 5-point harness conventional type CRS (using vehicle seat belt for installation) and 5-point harness ISOFIX CRS were developed and validated using frontal sled tests. The behavior and biomechanical responses of the Hybrid III dummy model and the child human FE model were compared and analyzed. Upper neck force and moment in the child human FE model were calculated based on the head motion and compared to those in the Hybrid III dummy model. A top-tether force limiter was proposed to reduce the loadings to the head, neck and chest of a child positioned in the ISOFIX CRS. For evaluating the effectiveness of the top-tether force limiter, FE simulations for two conditions, CRS in proper use and CRS harness having slack, were performed. Ridedown and restraint efficiencies for the chest of the Hybrid III dummy and child human FE model were analyzed and compared between the conventional type of 5-point harness CRS and the ISOFIX CRS in different using conditions.

2 METHODS

2.1 Sled tests and FE simulations

In this research, Frontal sled tests and FE simulations were conducted according to the ECE R44 sled test specification. The dummy used was not TNO P3 dummy prescribed in ECE R44, but a Hybrid III 3YO dummy. The acceleration pulse is shown in Figure 1. FE model (Figure 2) consists of an ECE seat, a 5-point harness CRS (conventional type or ISOFIX type) and a Hybrid III 3YO dummy FE model developed by FTSS (First Technology Safety System) or the child human FE model developed by Mizuno et al. [14, 15, 16]. To simulate the sliding of the shoulder harness and lap harness through the slip ring of the buckle, shell seat belt elements were used in the connection area of the shoulder harness and lap harness around the slip ring.

Table 1 presents the matrix of the sled tests and FE simulations. In Case A, the 5-point harness conventional type CRS was installed to the ECE seat by vehicle three-point seat belt in proper use condition. In Case B1 and C1, the 5-point harness CRS was installed by ISOFIX system, and in Case C1 100 mm slack was added to the CRS harness to simulate the typical misuse condition. Case A, B1 and C1 were conducted for both test and FE simulation. Case B2 and C2 with a force limiter in the top tether were done by FE simulation only. Table 2 lists the injury assessment reference values (IARVs) for a 3-year-old child used in this research, which are referred from ECE R44 and Mertz [17]. For the child human FE model, the upper neck shear and axial force are calculated based on the head motion [18].

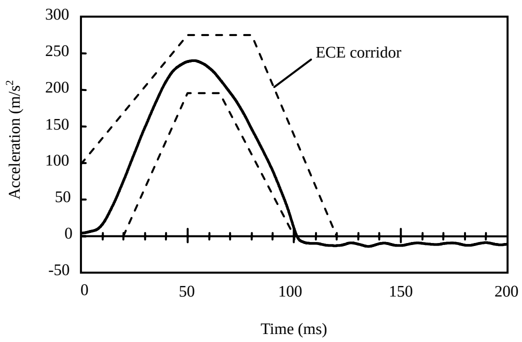

Figure 1 Acceleration pulse in sled test according to ECE R44

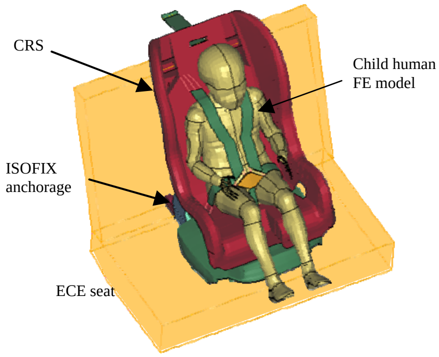

Figure 2 FE simulation model

Table 1 Sled tests and FE simulations matrix

Sled test	FE Simulation	Description
Case A	Case A	5-point harness CRS installed by vehicle seat belt (proper use)
Case B1	Case B1	ISOFIX CRS (proper use)
	Case B2	ISOFIX+ top-tether force limiter
Case C1	Case C1	ISOFIX with 100 mm harness slack (misuse)
	Case C2	ISOFIX with 100 mm harness slack + top-tether force limiter

Table 2 Injury assessment reference values (IARVs) for a 3-year-old child

Injury criteria	Head excursion	HIC 15	Upper neck shear force Fx	Upper neck tension force Fz	Upper neck flexion moment +My	Upper neck extension moment -My	Chest acceleration 3 ms
Value	550 mm	570	1070 N	1430 N	42 Nm	21 Nm	539 m/s^2

2.2 Ridedown and Restraint Efficiencies

In a vehicle frontal crash, an occupant's kinetic energy is dissipated by two processes: one is during occupant ridedown when the front end of the vehicle deforming in the crash and the other is during the occupant being restrained by restraint systems [19]. In distance domain these two processes can be regards as two independent processes, then the energy density of an occupant, *e*, can be expressed as:

$$e = \int a_o dx_o = \int a_o d(x_v + x_o - x_v) = e_{rd} + e_{rs} \tag{1}$$

where

$$\text{ridedown energy density: } e_{rd} = \int a_o dx_v \tag{2}$$

$$\text{restraint energy density: } e_{rs} = \int a_o d(x_o - x_v) \tag{3}$$

x_v: vehicle displacement relative to the ground
x_o: occupant displacement relative to the ground
x_o-x_v: occupant displacement relative to the vehicle
a_o: occupant acceleration

Ridedown and restraint efficiencies (μ_{rd} and μ_{rs}) are defined as the ratio of maximum ridedown and restraint energy densities to the initial occupant kinetic energy density as follows:

$$\mu_{rd} = \frac{e_{rd}\big|_{\max}}{\frac{1}{2}v_0^{\ 2}} \tag{4}$$

$$\mu_{rs} = \frac{e_{rs}\big|_{\max}}{\frac{1}{2}v_0^{\ 2}} \tag{5}$$

where v_0 is the vehicle initial velocity. The ECE R44 sled test is to simulate a frontal crash at a velocity difference of 50 km/h, accordingly, the initial energy density is 96.5 m^2/s^2.

3 RESULTS

3.1 Comparison of the behavior and responses of the Hybrid III dummy model and the child human model in ISOFIX CRS (Case B1)

Kinematics of the Hybrid III dummy and the child human FE model in the ISOFIX CRS (Case B1) are shown in Figure 3. As the upper part of the ISFOFIX CRS seatback was tensed by the top tether, the torso of the Hybrid III dummy showed a lying posture, while the torso of the human model showed more upright posture due to its whole spine flexion. At 100 ms the head rotated and moved to the lowest position. For the Hybrid III dummy model, only the cervical spine and lumber spine flexed, the thoracic spine did not bend since it is made of a steel box, then only the chin contacted with the chest. While for the human model the whole spine flexed so greatly that not only the mandible but the lower face made contact with the sternum. In the rebound phase, the Hybrid III dummy's head rotated upward greatly, and finally it made contact with the CRS seatback (150 ms) while the human's head only rotated upward slightly and the chin continued to contact the chest.

0 ms 60 ms 70 ms 100 ms 150 ms

Figure 3 Kinematics of Hybrid III dummy (upper) and human model (lower) in ISOFIX CRS (Case B1)

The tension force in the shoulder harness and the contact force of the chin and chest are shown in Figures 4 and 5. The head and chest accelerations, and the upper neck force and moment are shown in Figures 6 and 7, respectively. For both the Hybrid III dummy model and the child human FE model, at about 60 ms when the tension force in the shoulder harness reached the peak (Figure 4), the chest x acceleration also reached the peak (Figure 6c). At 70 ms, the chin contacted with the chest and the contact force started to increase (Figure 5) which resulted in a small decrease in the head x acceleration (Figure 6a) and the upper neck shear and tension force (Figure 7(a) (b)) for both models. When the contact force of the chin and chest reached the peak at about 80 ms (Figure 5), the head x acceleration (Figure 6a), the upper neck shear and tension force (Figure 7(a) (b)) reached their peaks for both models.

Figure 8 shows the equilibrium of the force sustained by the head when it contacted with the chest. For the Hybrid III dummy model, the chin-chest contact force in local x direction of the head coordinate system was very small (Figure 5) due to little displacement of the head relative to the chest in local x direction (Figure 8a). Since the contact force in local x direction was small, the head x acceleration was reflected by the upper neck shear force (see Figures 6a, 7a and 8a). While the contact force in local z direction was large because the chin contacted with the lower neck which is a rigid component (Figure 8a). For the child human FE model, the chin-chest contact force in local x direction and in local z direction were comparable, because the chin made contact with the flexible sternum which deformed in both local x and z directions (Figure 8b). As the head of the human model moved downward relative to the chest, the chin sustained a posterior force from the chest, which mitigated the upper neck shear force (Figures 8b). Although the contact force in local z direction for the Hybrid III dummy model was larger than that of the human model, as the head of the human model flexed downward much more greatly than the Hybrid III dummy model (Figure 8), the head inertial force of the human model in local z direction was larger than that of the Hybrid III dummy model (see Figure 6b). Accordingly, the peak upper neck tension force of the human model was comparable to that of the Hybrid III dummy model (Figure 7b).

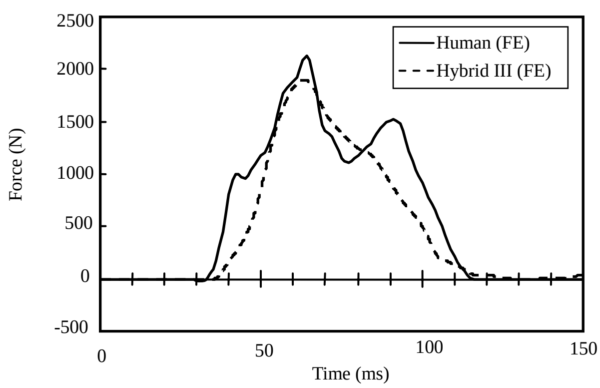

Figure 4 Tension force in the shoulder harness in ISOFIX CRS (Case B1)

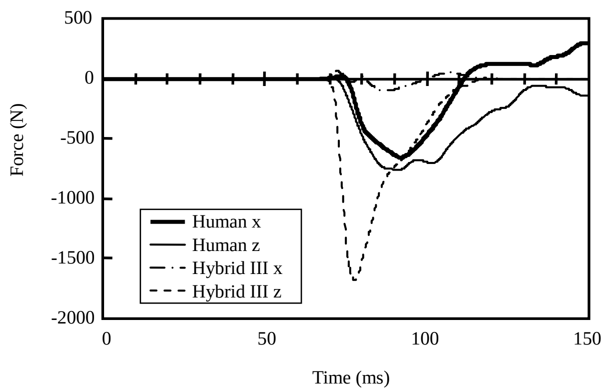

Figure 5 Chin-chest contact force of Hybrid III dummy and human model in ISOFIX CRS with respect to the head coordinate system (Case B1)

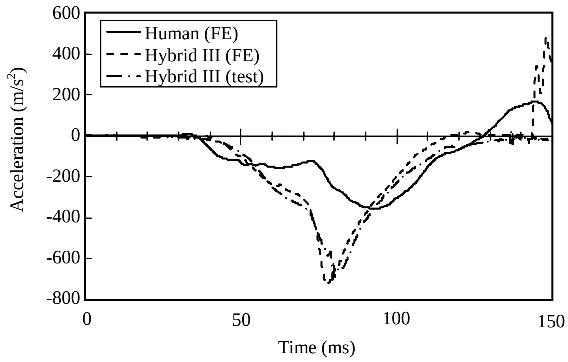

(a) Head acceleration (x)

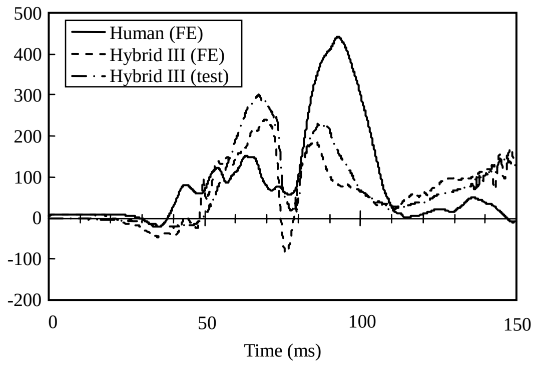

(b) Head acceleration (z)

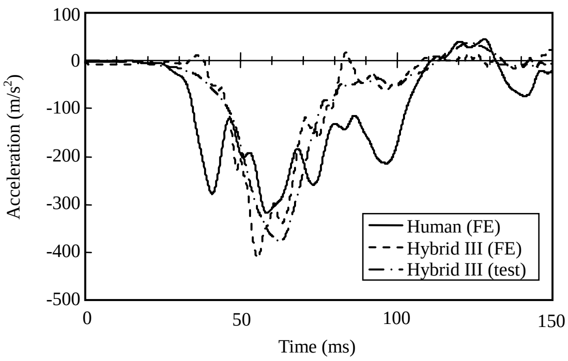

(c) Chest acceleration (x)

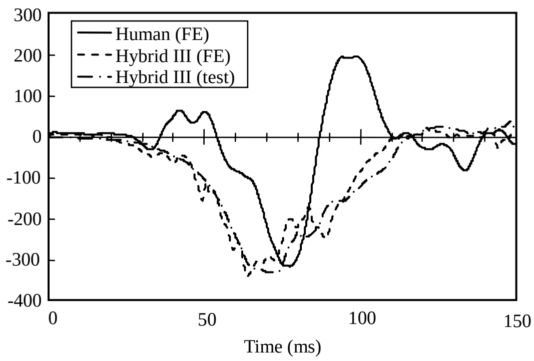

(d) Chest acceleration (z)

Figure 6 Head and chest acceleration of Hybrid III dummy and human model in ISOFIX CRS (Case B1)

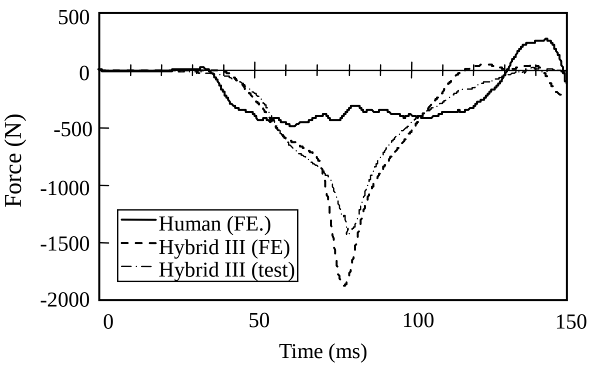

(a) Shear force

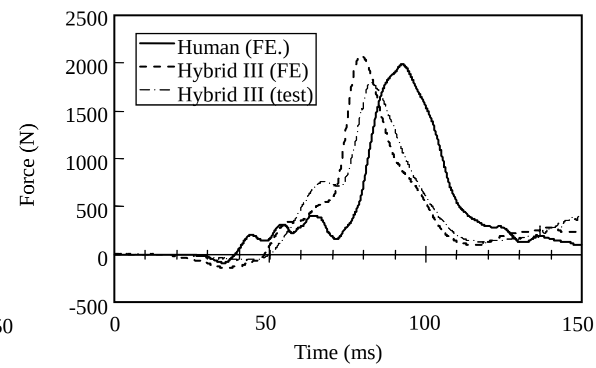

(b) Tension force

Figure 7 Upper neck force and moment in ISOFIX CRS (Case B1)

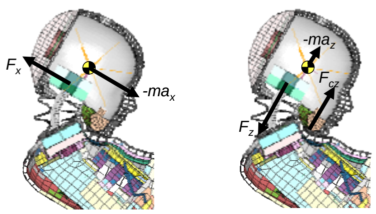

(a) Hybrid III 3YO

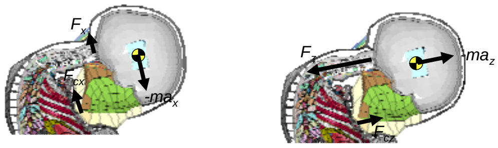

(b) Child human FE model

Figure 8 Equilibrium of head forces for Hybrid III dummy model and human model in ISOFIX CRS (Case B1)

3.2 Effect of a top-tether force limiter

A top-tether force limiter is expected to reduce the head and chest acceleration and the neck force and moment by allowing the displacement of the upper part of the ISOFIX CRS seatback. In the present research, the maximum force of the force limiter was set as 1200 N which was about half of the peak tension force in the top tether when the ISOFIX CRS was in proper use.

Due to the top-tether force limiter, the CRS moves forward with pitch motion (Case B2). The torso of both the Hybrid III dummy and the child human model shows an upright posture in Case B2 compared with that in Case B1.

From Figures 9 and 10, it was found that except the head excursion, all injury criteria were decreased. Especially in the misuse condition (100 mm harness slack), for the Hybrid III dummy model both the chest acceleration and the upper neck extension moment were reduced to be below the IARVs, and the upper neck shear and tension force were reduced to be comparable with the IARVs (Figure 9b). For the human model, the upper neck tension force was reduced to be below the IARVs (Figure 10b).

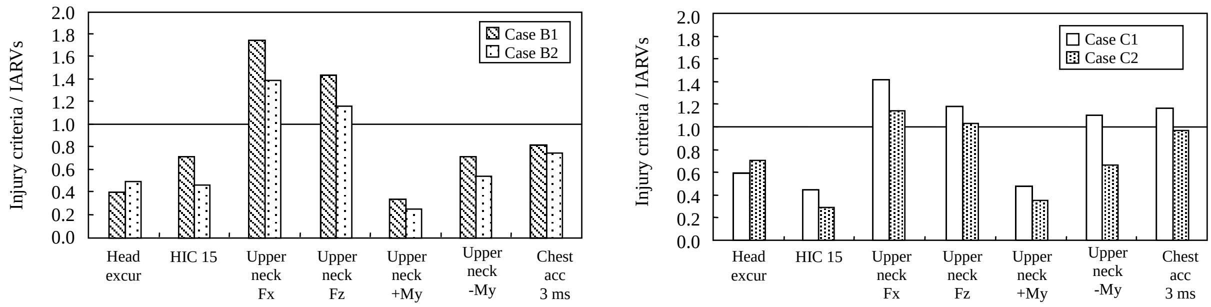

(a) Without harness slack

(b) With harness slack 100 mm

Figure 9 Ratios of injury criteria for Hybrid III 3YO in ISOFIX CRS with (Case B2 and C2) and without (Case B1 and C1) a top-tether force limiter for with and without harness slack

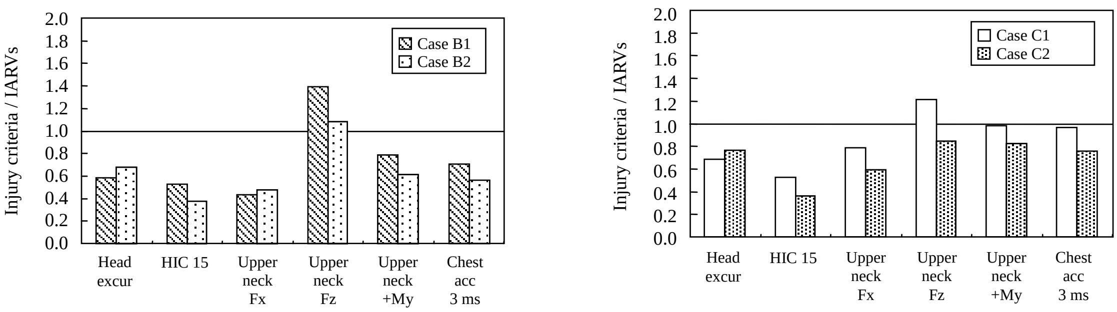

(a) Without harness slack

(b) With harness slack 100 mm

Figure 10 Ratios of injury criteria for child human model in ISOFIX CRS with (Case B2 and C2) and without (Case B1 and C1) a top-tether force limiter for with and without harness slack

3.3 Energy efficiency

To examine the differences of the chest acceleration level between the conventional type CRS and the ISOFIX CRS in different using conditions, the ridedown and restraint efficiencies were calculated. The energy efficiencies related with the CRS harness $\mu_{rs(harness)}$ and the CRS installation device $\mu_{rs(CRS)}$, the sum of which was the restraint efficiency μ_{rs}, were also calculated. The results are listed in Table 3. Note that the sum of μ_{rd}, $\mu_{rs(CRS)}$ and $\mu_{rs(harness)}$, is close to 100%, which means that the sum of the ridedown energy, and the energy related with the CRS installation device and the CRS harness is equivalent to the initial occupant kinetic energy.

By comparing the case of the conventional type CRS (Case A) and the proper use ISOFIX CRS (Case B1) for the Hybrid III dummy model, although ridedown energy efficiency μ_{rd} in Case A (51.3%) was much lower than that in Case B1 (80.4%), the energy efficiency related with the CRS installation device $\mu_{rs(CRS)}$ was much higher in Case A (38.6%) than that in Case B1 (12.3%). This is because for the conventional type CRS the seat belt absorbed much more energy compared to the ISOFIX anchorage and top tether. As a result, the energy absorption efficiency of the CRS harness $\mu_{rs(harness)}$ was comparable in Case A (10.6%) and Case B1 (9.6%), and consequently, the chest acceleration level was similar in these two cases.

For the cases without and with force limiter in ISOFIX proper use condition (Case B1 and B2) and with harness slack (Case C1 and C2) for both the Hybrid III dummy model and the human model, the ridedown efficiency μ_{rd} decreased due to the top-tether force limiter (Case B2 and C2). However, the energy efficiency related with the CRS installation device $\mu_{rs(CRS)}$ increased, and the energy absorption efficiency of CRS harness $\mu_{rs(harness)}$ was decreased. Consequently the chest acceleration were reduced in the cases with force limiter (Case B2 and C2) compared to the cases without force limiter (Case B1 and C1). Comparing the cases without harness slack and with harness slack (Case B1 and C1) for both the Hybrid III dummy model and the human model, the ridedown efficiency μ_{rd} decreased due to harness slack. The energy absorption efficiency of CRS harness $\mu_{rs(harness)}$ increased due to the larger forward movement of the torso, and consequently, the chest acceleration increased.

The relation between the chest energy efficiency and the chest acceleration is shown in Figure 11. The chest acceleration does not relate directly with the ridedown energy efficiency, but depends on the energy absorption efficiency of the CRS harness. When the energy efficiency of CRS harness increases the chest acceleration increases.

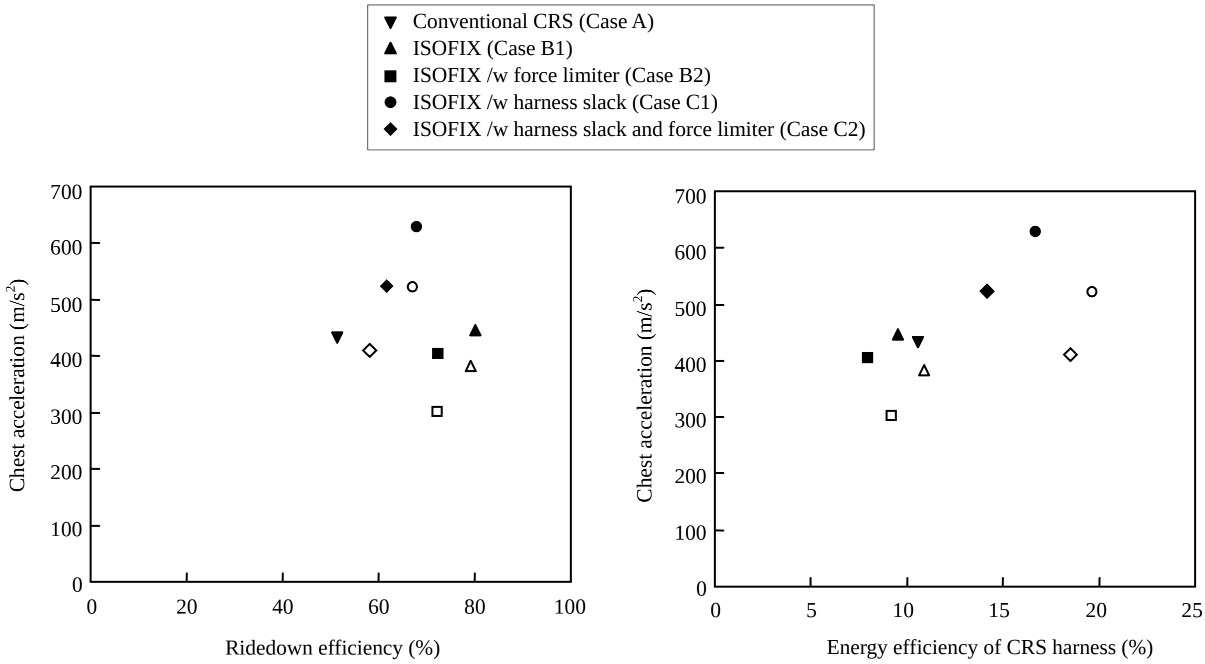

(a) Ridedown energy and chest acceleration (b) CRS harness energy and chest acceleration

Figure 11 Relation between the energy efficiencies and the chest acceleration. Closed symbols are Hybrid III 3YO FE model and open symbols are child human FE model.

Table 3 Energy efficiencies for the chest of Hybrid III dummy and human model

	Hybrid III dummy FE model				Child human FE model			
	μ_{rd}	μ_{rs}: $\mu_{rs(CRS)}$	μ_{rs}: $\mu_{rs(harness)}$	Chest acceleration 3 ms (m/s^2)	μ_{rd}	μ_{rs}: $\mu_{rs(CRS)}$	μ_{rs}: $\mu_{rs(harness)}$	Chest acceleration 3 ms (m/s^2)
Case A	51.3	38.6	10.6	433				
Case B1	80.4	12.3	9.6	444	79.4	9.4	11.3	380
Case B2	72.5	20.0	8.0	407	72.0	19.0	9.0	304
Case C1	68.0	16.2	16.7	629	67.2	13.3	19.9	521
Case C2	61.7	24.3	14.2	523	58.0	23.9	18.2	410

4 CONCLUSIONS

In the present research, the behavior and responses were examined for both the Hybrid III 3YO dummy and the child human FE model. The results were summarized as:

- The thoracic spine of the Hybrid III dummy model is a steel box while the child human FE model has a flexible thoracic spine. Accordingly, the chin-chest contact behavior was different between the two models. Due to the different chin-chest contact force and head inertial force, the Hybrid III dummy model showed a large upper neck shear force and tension force, while the child human model showed a large upper neck tension force.
- In the present research, since the child was seated in the CRS seat, the restraint energy was considered to be consisted of two parts: the energy dissipated into the CRS installation device and the energy absorbed by the CRS harness. The energy absorption efficiency of CRS harness has a direct relation with the chest acceleration. The lower energy efficiency of CRS harness for the chest means the lower chest acceleration. The energy efficiency of the CRS harness for the chest was similar between the ISOFIX CRS and the conventional type CRS, because the ridedown energy was larger in the ISOFIX CRS and the energy absorbed by the vehicle seat belt in the conventional type CRS was larger compared to the ISOFIX anchorage and top tether. As a result, the chest acceleration peaks in the two types of CRSs were comparable.
- A top-tether force limiter proved to be effective. The torso of the child showed an upright posture in the ISOFIX CRS with a top-tether force limiter. Head and chest accelerations and upper neck force and moment were decreased for both the Hybrid III dummy model and the human model, although the head excursion increased slightly but still below the IARV.

REFERENCES

[1] National Highway Traffic Safety Administration. Traffic Safety Facts 2006, Children, Available at http://www.nhtsa.dot.gov/ Accessed May 1, 2008.
[2] Langwieder, K., Hummel, T., Roselt, T., ISOFIX-possibilities and problems of a new concept for child restraint systems, IJCrash, Vol. 8, No. 5, pp. 443-454, 2003.
[3] Arbogast, K., Durbin, D., Cornejo, R., Kallan, M., Winston, F., An evaluation of the effectiveness of forward facing child restraint systems, Accident Analysis & Prevention, 36, pp. 585-589, 2004.
[4] National Highway Traffic Safety Administration. Traffic Safety Facts, Misuse of Child Restraints: Results of A Workshop to Review Field Data Results, Available at http://www.nhtsa.dot.gov/ Accessed December 1, 2007.
[5] Lang, H., ISOFIX-Current Status, ROSPA-Conference 2003.
[6] Weber, K., Crash Protection for Child Passengers, UMTRI Research Review, July-September 2000, Vol.31, No.3.
[7] Scherz, R., Epidemiology of Childhood Motor Vehicle Related Accidents, SAE 791013, 1979.
[8] Fuchs, S., Barthel, M., Flannery, A., Christoffel, K., Cervical Spine Fractures Sustained by Young Children in Forward-Facing Car Seats, PEDIATRICS, Vol. 84, No. 2, August 1989.
[9] Sochor, M., Faust, D., Garton, H., Wang, S., Ridella, S., Barnes, S., Fischer, K., Simulation of Occipitoatlantoaxial Injury Utilizing a MADYMO Model, SAE 2004-01-0326, 2004.
[10] De Jager, K., van Ratingen, M., Lesire, P., Guillemot, H., Pastor, C., Schnottale, B., Tejera, G., Lepretre, J., Assessing New Child Dummies and Criteria for Child Occupant Protection in Frontal Impact, EEVC 05-0157.
[11] Hoy, G., Cole, W., The paediatric cervical seat belt syndrome, Injury, 24, (5), 1993.
[12] van Rooij, L., Sherwood, C., Crandall, J., Orzechowski, K., Eichelberger, M., The Effects of Vehicle Seat Belt Parameters on the Injury Risk for Children in Booster Seats, SAE 2003-01-0500, 2003.
[13] Mertz, H., Horsch, J., Horn, G., Lowne, R., Hybrid III Sternal Deflection Associated with Thoracic Injury Severities of Occupants Restrained with Force-Limiting Shoulder Belts, SAE 910812, 1991.
[14] Mizuno, K., Namikiri T., Analysis of Child Responses in CRS using Child Human FE Model, ESV 07-0145.
[15] Mizuno, K., Iwata, K., Deguchi, T., Kubota, M., Development of a three-year-old child FE model, Traffic Injury Prevention, Vol. 6, Issue 4, pp. 361-371, 2005.
[16] Mizuno, K., Iwata, K., Namikiri T., Tanaka, N., Comparison of human FE model and crash dummy response in various child restraint systems, ICRASH 2006, Athens, Greece.
[17] Mertz, H., Irwin, A., Biomechanical and Scaling Bases for Frontal and Side Impact Injury Assessment Reference Values, SAE 2003-22-0009.
[18] Mertz, H., Patrick, L., Strength and Response of the Human Neck, SAE 710855, 1971.
[19] Huang, M., *Vehicle Crash Mechanics*, CRC Press, 2002.